Rapid estimation of elastic constants by molecular dynamics simulation under constant stress

Wataru Shinoda,[1,*] Motoyuki Shiga,[2] and Masuhiro Mikami[1]
[1]*Research Institute for Computational Sciences, National Institute for Advanced Industrial Science and Technology (AIST), Central 2, 1-1-1 Umezono, Tsukuba, Ibaraki 305-8568, Japan*
[2]*Center for Promotion of Computational Science and Engineering, Japan Atomic Energy Research Institute, 6-9-3 Higashi-Ueno, Taito-ku, Tokyo 110-0015, Japan*
(Received 4 November 2003; published 7 April 2004)

Molecular simulations, when they are used to understand properties characterizing the mechanical strength of solid materials, such as stress-strain relation or Born stability criterion, by using elastic constants, are sometimes seriously time consuming. In order to resolve this problem, we propose an efficient simulation approach under constant external stress and temperature, modifying Parrinello-Rahman (PR) method using useful sampling techniques developed recently—massive Nosé-Hoover chain method and hybrid Monte Carlo method. Test calculations on the Ni crystal employing the embedded atom method have shown that our method greatly improved the efficiency in sampling the elastic properties compared with the conventional PR method.

DOI: 10.1103/PhysRevB.69.134103 PACS number(s): 62.20.Dc

I. INTRODUCTION

Molecular simulation in the presence of external stress is important as it is related to the mechanical strength of solid materials such as metals, ceramics, and amorphous polymers.[1–5] One of the goals of such a simulation will be direct calculation of stress-strain curve and determination of the yield point by the Born stability criteria using the calculated elastic constants.[5–11] As a useful approach to this aim, Parrinello and Rahman (PR) have suggested a molecular dynamics (MD) under the $N\mathbf{t}H$ ensemble in which the simulation cell containing N atoms allows us to change its shape appropriately conforming to external stress $\mathbf{t}$ (strictly speaking, this should be referred to as ''thermodynamic tension''[6]) and enthalpy H.[7,8,12] However, it is well known that a simple PR approach would be somewhat problematic for the evaluation of the elastic constants, since the MD calculations of elastic constants are usually time consuming.[6,13] Even for the zero-stress case, a satisfactorily converged result for the elastic constants might take a simulation run of typically several millions or more sampling steps. To resolve this problem, we propose a MD-based simulation algorithm to estimate thermodynamic properties for the $N\mathbf{t}T$ ensemble when the stress $\mathbf{t}$ is nonzero, using the efficient sampling techniques developed to attain the canonical distribution rapidly.[14,15] Here, the equation of motion in non-Hamiltonian dynamics[16–18] is solved by time-reversible RESPA algorithm.[19,20] This formulation enables us to consider various methods in system-thermostat coupling,[14,21,22] so that the system temperature is efficiently controlled. In the present work, we employ three types of thermostat, i.e., Nosé-Hoover (NH),[21,22] Nosé-Hoover chain (NHC),[14] and massive Nosé-Hoover chain (MNHC), and their sampling efficiency of the lattice constants and elastic constants are examined. In addition, the time reversibility in this algorithm allows us to use hybrid Monte Carlo[15] (HMC) method in the $N\mathbf{t}T$ ensemble. The efficiency of HMC method is also compared with other methods. A series of test calculations are performed for Ni crystal, where embedded atom method[23,24] (EAM) is used for interatomic interactions.

There has been a lot of effort devoted to the method for accurate evaluation of elastic constants by MD or Monte Carlo (MC) simulations.[2,3,5,9,10,26–31] While most of the calculations are limited to elastic constants in zero-stress condition, it is worthwhile to briefly describe this topic. The simplest method would be to impose a strain on the sample and calculate the corresponding strain energy or stress by the standard $N\mathbf{h}E$ ensemble MD where the energy E and cell matrix $\mathbf{h}$ are constants, and then calculate the elastic constants from the stress-strain relationship.[6,13] However, it is inconvenient because several strains must be imposed at several times to calculate all the elastic constants. Besides, numerical error in finite-difference differentiation would be inevitable. Elastic constants can also be calculated by the standard $N\mathbf{h}E$ ensemble MD in another way, based on the fluctuation theory that microscopic stress tensor and first and second derivatives of the potential are related to elastic constants.[6] Although $N\mathbf{h}E$ MD calculation usually gives good convergence and accurate results, it is rarely used in the simulations for system beyond pair potential[6,27,31] (e.g., many-body potentials or first-principles potential) except in some cases,[2,3] or Coulombic system in which Ewald summation is needed, since the second derivatives of the potential (Born term) are uneasy to calculate. Another difficulty is that the stress cannot be controlled using a rigid cell $\mathbf{h}$. As another way, elastic constants can be obtained from MD or MC methods based on flexible-cell $N\mathbf{t}H$ ensemble by the calculation of strain fluctuations. Although these methods are promising, it has been reported that the statistical convergence is unsatisfactory in some systems which may be due to nonergodicity problem.[6,13] These are the motivations to develop a MD approach based on $N\mathbf{t}T$ ensemble for which some efficient sampling techniques are available with a combination of thermostat and barostat.

This paper is organized as follows. In Sec. II, we describe the equation of motion and RESPA integrator[19] for $N\mathbf{t}T$ ensemble based on non-Hamiltonian dynamics as an extension of the formulation previously suggested by Martyna and Tuckerman,[16–18] along with hybrid Monte Carlo algorithm following the formulation by Mehlig *et al.*[15] In Sec. III, the

conditions and results of the test calculation of Ni crystal are described. Finally, this paper ends with a discussion on the methodological aspects in Sec. IV.

II. METHODS

As mentioned above, we consider here an efficient sampling scheme for evaluating elastic constants by using a molecular dynamics simulation under constant stress and constant temperature based on the $N\mathbf{t}T$ ensemble. The non-Hamiltonian MD techniques were employed to generate the $N\mathbf{t}T$ ensemble. The $N\mathbf{t}H$-MD was also used in the hybrid Monte Carlo simulation. In this section, MD and HMC algorithms used in our examination are described in detail.

A. Molecular dynamics

As a barostat, the fully flexible cell with a modular invariant form of the momentum was employed to control the internal stress.[18] For the temperature control, we considered three different choices in the method of thermostat coupling: Nosé-Hoover,[22] Nosé-Hoover chain, and massive Nosé-Hoover chain.[14] By setting up these types of barostat and thermostat, stable integrators can be straightforwardly constructed for the extended system dynamics on the basis of the Trotter factorization of the Liouville operator by the reversible RESPA algorithm.[19] Here, as an example, the equations of motion (EOM) for the case of NHC are given by

$$\dot{\mathbf{r}}_i=\frac{\mathbf{p}_i}{m_i}+\frac{\mathbf{p}_g}{W_g}\mathbf{r}_i,$$

$$\dot{\mathbf{p}}_i=\mathbf{F}_i-\frac{\mathbf{p}_g}{W_g}\mathbf{p}_i-\frac{1}{N_f}\frac{\mathrm{Tr}[\mathbf{p}_g]}{W_g}\mathbf{p}_i-\frac{p_\xi}{Q}\mathbf{p}_i,$$

$$\dot{\mathbf{h}}=\frac{\mathbf{p}_g}{W_g}\mathbf{h},$$

$$\dot{\mathbf{p}_g}=V(\mathbf{P}_{\mathrm{int}}-\mathbf{I}P_{\mathrm{ext}})-\mathbf{h}\Sigma\mathbf{h}^t+\left(\frac{1}{N_f}\sum_{i=1}^{N}\frac{\mathbf{p}_i^2}{m_i}\right)\mathbf{I}-\frac{p_{\xi_1}}{Q_1}\mathbf{p}_g,$$

$$\dot{\xi}_k=\frac{p_{\xi_k}}{Q_k}\quad\text{for}\quad k=1,\ldots,M,$$

$$\dot{p}_{\xi_1}=\sum_{i=1}^{N}\frac{\mathbf{p}_i^2}{m_i}+\frac{1}{W_g}\mathrm{Tr}[\mathbf{p}_g^t\mathbf{p}_g]-(N_f+d^2)kT_{\mathrm{ext}}-p_{\xi_1}\frac{p_{\xi_2}}{Q_2},$$

$$\dot{p}_{\xi_k}=\left(\frac{p_{\xi_{k-1}}^2}{Q_{k-1}}-kT_{\mathrm{ext}}\right)-p_{\xi_k}\frac{p_{\xi_{k+1}}}{Q_{k+1}}\quad\text{for}\quad k=2,\ldots,M-1,$$

$$\dot{p}_{\xi_M}=\left(\frac{p_{\xi_{M-1}}^2}{Q_{M-1}}-kT_{\mathrm{ext}}\right),\tag{1}$$

where variables $\{\mathbf{r}_i,\mathbf{p}_i\}$ are the position and momentum of atom i, $\mathbf{h}$ is the cell matrix, $\mathbf{p}_g$ is the modularly invariant form of the cell momenta, and $\{\xi_k,p_{\xi k}\}$ are the thermostat variable and its conjugated momentum of the $k$sth thermostat of the NHC (length $=M$), respectively. The constants m_i, W_g, and Q_k are the mass of atom i, barostat, and kth thermostat, respectively, and the latter two were used to tune the frequency at which those variables fluctuate.[20] The constant N_f $(=3N)$ is the number of system degrees of freedom and the tensor $\mathbf{I}$ denotes the identity matrix. The parameter T_{ext} is the external temperature and the parameter P_{ext} is the hydrostatic pressure, and the internal pressure $\mathbf{P}_{\mathrm{int}}$ is defined as,

$$(P_{\mathrm{int}})_{\alpha\beta}=\frac{1}{V}\left\{\sum_{i=1}^{N}\frac{(\mathbf{p}_i)_\alpha(\mathbf{p}_i)_\beta}{m_i}+(\mathbf{F}_i)_\alpha(\mathbf{r}_i)_\beta-(\boldsymbol{\phi}'\mathbf{h}^t)_{\alpha\beta}\right\},$$

$$(\phi')_{\alpha\beta}=\frac{\partial\phi(\mathbf{r},\mathbf{h})}{\partial(h)_{\alpha\beta}}.\tag{2}$$

The matrix $\boldsymbol{\Sigma}$ is defined by

$$\boldsymbol{\Sigma}=\mathbf{h}_0^{-1}(\mathbf{t}-\mathbf{I}P_{\mathrm{ext}})\mathbf{h}_0^{t\,-1},\tag{3}$$

where $\mathbf{t}$ is the stress applied to the system. The above equations of motions have the conserved quantity,

$$H'=\sum_{i=1}^{N}\frac{\mathbf{p}_i^2}{2m_i}+\frac{1}{2W_g}\mathrm{Tr}[\mathbf{p}_g^t\mathbf{p}_g]+\sum_{k=1}^{M}\frac{p_{\xi_k}^2}{2Q_k}+\phi(\mathbf{r},\mathbf{h})+P_{\mathrm{ext}}\det[\mathbf{h}]+\frac{1}{2}\mathrm{Tr}[\mathbf{h}_0^{-1}(\mathbf{t}-\mathbf{I}P_{\mathrm{ext}})\mathbf{h}_0^{t\,-1}\mathbf{G}]+(N_f+d^2)kT_{\mathrm{ext}}\xi_1+\sum_{k=2}^{M}kT_{\mathrm{ext}}\xi_k,\tag{4}$$

where $\mathbf{G}=\mathbf{h}^t\mathbf{h}$ is the metric tensor, and the sixth term in right-hand side of the above equation denotes the elastic energy due to the external stress.

The Jacobian of the coordinate transformation is calculated as[18]

$$J=\det[\mathbf{h}]^{1-d}\exp\left[(N_f+d^2)\xi_1+\sum_{k=2}^{M}\xi_k\right].\tag{5}$$

This leads us to find the partition function as

$$\Delta\propto\int d\mathbf{h}\exp[-\beta H'']\det[\mathbf{h}]^{1-d},\tag{6}$$

where

$$H''=\sum_{i=1}^{N}\frac{\mathbf{p}_i^2}{2m_i}+\frac{1}{2W_g}\mathrm{Tr}[\mathbf{p}_g^t\mathbf{p}_g]+\sum_{k=1}^{M}\frac{p_{\xi_k}^2}{2Q_k}+\phi(\mathbf{r},\mathbf{h})+P_{\mathrm{ext}}\det[\mathbf{h}]+\frac{1}{2}\mathrm{Tr}[\mathbf{h}_0^{-1}(\mathbf{t}-\mathbf{E}P_{\mathrm{ext}})\mathbf{h}_0^{t\,-1}\mathbf{G}].\tag{7}$$

Taking $M=1$ in EOM (1), we obtain NH-MD instead of NHC-MD. In case of MNHC-MD, all the system degrees of freedom $(=3N)$ and all the degrees of freedom in the cell matrix $(=6$, without rotation) are separately coupled with the respective Nosé-Hoover chains. It should be noted that, to eliminate the rotation of the cell, the off-diagonal elements of the cell momentum matrix were $(\mathbf{p}_g)_{\alpha\beta}=(\mathbf{p}_g)_{\beta\alpha}$, and

their kinetic energy $\{(\mathbf{p}_g)_{\alpha\beta}^2+(\mathbf{p}_g)_{\beta\alpha}^2\}/2W_g$ is controlled to $kT_{\text{ext}}/2$ (not kT_{ext}). An explicit reversible integrator was constructed on the basis of the rRESPA algorithm and employed to generate the $N\mathbf{t}T$ dynamics.[20] Now, there are several choices of the factorization scheme of the time evolution operator. In this work, we used the following form:

$$\exp(iL\Delta t)=\exp\left(iL_{\text{bath}}\frac{\Delta t}{2}\right)\exp\left(iL_2\frac{\Delta t}{2}\right)\exp(iL_1\Delta t)\times\exp\left(iL_2\frac{\Delta t}{2}\right)\exp\left(iL_{\text{bath}}\frac{\Delta t}{2}\right)+O(\Delta t^3), \tag{8}$$

where iL is the Liouville operator, which is decomposed into three components iL_1, iL_2, and iL_{bath}:

$$iL=iL_1+iL_2+iL_{\text{bath}},$$

$$iL_1=\sum_{i=1}^{N}[\mathbf{v}_i+\mathbf{v}_g\mathbf{r}_i]\cdot\boldsymbol{\nabla}_{\mathbf{r}_i}+\sum_{\alpha,\beta}(\mathbf{v}_g)_{\alpha\beta}\frac{\partial}{\partial(\mathbf{h})_{\alpha\beta}},$$

$$iL_2=\sum_{i=1}^{N}\left[\frac{\mathbf{F}_i}{m_i}\right]\cdot\boldsymbol{\nabla}_{\mathbf{v}_i}, \tag{9}$$

$$iL_{\text{bath}}=\sum_{i=1}^{N}\left[-\left\{\mathbf{v}_g+\left(\frac{1}{N_f}\right)\text{Tr}[\mathbf{v}_g]+v_{\xi_1}\right\}\mathbf{v}_i\right]\cdot\boldsymbol{\nabla}_{\mathbf{v}_i}+\sum_{\alpha,\beta}\left\{\frac{1}{W_g}\left[\sum_{i=1}^{N}m_i(\mathbf{v}_i)_\alpha(\mathbf{v}_i)_\beta+\sum_{i=1}^{N}(\mathbf{F}_i)_\alpha(\mathbf{r}_i)_\beta-(\boldsymbol{\phi}'\mathbf{h}^t)_{\alpha\beta}\right.\right.$$
$$\left.+\left(\frac{1}{N_f}\sum_{i=1}^{N}m_i\mathbf{v}_i^2-P_{\text{ext}}V\right)\delta_{\alpha\beta}-[\mathbf{h}\mathbf{h}_0^{-1}(\mathbf{t}-\mathbf{I}P_{\text{ext}})\mathbf{h}_0^{t^{-1}}\mathbf{h}^t]_{\alpha\beta}\right]-v_{\xi_1}(\mathbf{v}_g)_{\alpha\beta}\left.\right\}\frac{\partial}{\partial(\mathbf{v}_g)_{\alpha\beta}}+\sum_{k=1}^{M}v_{\xi_k}\frac{\partial}{\partial\xi_k}$$
$$+\left[\frac{1}{Q_1}\left(\sum_{i=1}^{N}m_i\mathbf{v}_i^2+W_g\text{Tr}[\mathbf{v}_g^t\mathbf{v}_g]-(N_f+d^2)kT_{\text{ext}}\right)-v_{\xi_1}v_{\xi_2}\right]\frac{\partial}{\partial v_{\xi_1}}$$
$$+\sum_{k=2}^{M-1}\left[\frac{1}{Q_k}(Q_{k-1}v_{\xi_{k-1}}^2-kT_{\text{ext}})-v_{\xi_k}v_{\xi_{k+1}}\right]\frac{\partial}{\partial v_{\xi_k}}+\left[\frac{1}{Q_M}(Q_{M-1}v_{\xi_{M-1}}^2-kT_{\text{ext}})\right]\frac{\partial}{\partial v_{\xi_M}}, \tag{10}$$

where $\mathbf{v}_i=\mathbf{p}_i/m_i\neq\dot{\mathbf{r}}_i$, $\mathbf{v}_g=\mathbf{p}_g/W_g$, and $v_{\xi_k}=p_{\xi_k}/Q_k$.

B. Hybrid Monte Carlo

Hybrid Monte Carlo method was originally used to generate $N\mathbf{h}T$ ensemble in Metropolis MC sampling utilizing the trajectories of $N\mathbf{h}E$ MD.[15] Now we want to apply this idea to obtain $N\mathbf{t}T$ trajectories utilizing $N\mathbf{t}H$ MD trajectories. The algorithm for $N\mathbf{t}H$ MD is very similar to that for $N\mathbf{t}T$ MD described above. The EOM for $N\mathbf{t}H$ MD are just the EOM's of $N\mathbf{t}T$ MD, Eq. (1), except that the terms related to the thermostat variables $\{\xi_k,p_{\xi_k}\}$ are not included. It should be noted that the Jacobian of the EOM is not unity but $J=\det[\mathbf{h}]^{1-d}$.[18] Therefore, to satisfy the detailed balance condition, the changes in the volume elements in the phase-space trajectory should be taken into account.

In the isothermal-isostress ensemble, the probability that the system is in a configuration $(\mathbf{r},\mathbf{h})$ is proportional to

$$\mathcal{N}(\mathbf{r},\mathbf{h})d\mathbf{r}d\mathbf{h}=\frac{\exp\{-\beta(\phi+P_{\text{ext}}\det[\mathbf{h}]+\frac{1}{2}\text{Tr}[\boldsymbol{\Sigma}\mathbf{G}])\}}{\Xi}d\mathbf{r}d\mathbf{h}, \tag{11}$$

where Ξ is the configurational integral,

$$\Xi=\int d\mathbf{r}d\mathbf{h}\exp\left\{-\beta\left(\phi+P_{\text{ext}}\det[\mathbf{h}]+\frac{1}{2}\text{Tr}[\Sigma\mathbf{G}]\right)\right\}. \tag{12}$$

The detailed balance condition can be written as

$$\mathcal{N}(\mathbf{r},\mathbf{h})P_M(\mathbf{r},\mathbf{h}\rightarrow\mathbf{r}',\mathbf{h}')d\mathbf{r}d\mathbf{h}d\mathbf{r}'d\mathbf{h}'=\mathcal{N}(\mathbf{r}',\mathbf{h}')P_M(\mathbf{r}',\mathbf{h}'\rightarrow\mathbf{r},\mathbf{h})d\mathbf{r}d\mathbf{h}d\mathbf{r}'d\mathbf{h}', \tag{13}$$

where $P_M(\mathbf{r},\mathbf{h}\rightarrow\mathbf{r}',\mathbf{h}')$ denotes the transition probability to go from configuration $(\mathbf{r},\mathbf{h})$ to $(\mathbf{r}',\mathbf{h}')$. In a MC algorithm, the transition matrix is given by

$$P_M(\mathbf{r},\mathbf{h}\rightarrow\mathbf{r}',\mathbf{h}')=p_s(\mathbf{r},\mathbf{h}\rightarrow\mathbf{r}',\mathbf{h}')P_{acc}(\mathbf{r},\mathbf{h}\rightarrow\mathbf{r}',\mathbf{h}'), \tag{14}$$

where $P_{acc}(\mathbf{r},\mathbf{h}\rightarrow\mathbf{r}',\mathbf{h}')$ denotes the probability of accepting a trial move from $(\mathbf{r},\mathbf{h})$ to $(\mathbf{r}',\mathbf{h}')$. In the HMC, as described above, MD is used to generate a trial move of the system with a probability $p_s(\mathbf{r},\mathbf{h}\rightarrow\mathbf{r}',\mathbf{h}')$. In order to meet the detailed balance condition, we have chosen the probability $p_s(\mathbf{r},\mathbf{h}\rightarrow\mathbf{r}',\mathbf{h}')$ to be a symmetric matrix, assigning to the initial momentum chosen from a Maxwellian distribution at T. Since the system is moved deterministically through phase space, p_s can be rewritten as

$$p_s(\mathbf{r},\mathbf{h}\rightarrow\mathbf{r}',\mathbf{h}')d\mathbf{r}'d\mathbf{h}'=p_s(\mathbf{p},\mathbf{p}_g)d\mathbf{p}^Nd\mathbf{p}_g. \tag{15}$$

Therefore, the acceptance probability has been taken as

$$P_{\rm acc}(\mathbf{r}^N,\mathbf{h}\rightarrow\mathbf{r}^{N'},\mathbf{h}') = \min\left\{1,\frac{\mathcal{N}(\mathbf{r}^{N'},\mathbf{h}')p_s(\mathbf{r}^{N'},\mathbf{h}'\rightarrow\mathbf{r}^N,\mathbf{h})d\mathbf{r}^N d\mathbf{h} d\mathbf{r}^{N'} d\mathbf{h}'}{\mathcal{N}(\mathbf{r}^N,\mathbf{h})p_s(\mathbf{r}^N,\mathbf{h}\rightarrow\mathbf{r}^{N'},\mathbf{h}')d\mathbf{r}^N d\mathbf{h} d\mathbf{r}^{N'} d\mathbf{h}'}\right\}$$

$$= \min\left\{1,\frac{\exp\left\{-\beta\left(\phi' + P_{\rm ext}\det[\mathbf{h}'] + \frac{1}{2}\mathrm{Tr}[\Sigma\mathbf{G}']\right)\right\}p_s(\mathbf{p}^{N'},\mathbf{p}_g')d\mathbf{r}^{N'}d\mathbf{h}'d\mathbf{p}^{N'}d\mathbf{p}_g'}{\exp\left\{-\beta\left(\phi + P_{\rm ext}\det[\mathbf{h}] + \frac{1}{2}\mathrm{Tr}[\Sigma\mathbf{G}]\right)\right\}p_s(\mathbf{p}^N,\mathbf{p}_g)d\mathbf{r}^N d\mathbf{h} d\mathbf{p}^N d\mathbf{p}_g}\right\}$$

$$= \min\{1,\exp[-\beta(H_1'-H_1)]J(\mathbf{r}^{N'},\mathbf{h}',\mathbf{p}^{N'},\mathbf{p}_g';\mathbf{r}^N,\mathbf{h},\mathbf{p}^N,\mathbf{p}_g)\}$$

$$= \min\left\{1,\exp[-\beta(H_1'-H_1)]\frac{\sqrt{g}}{\sqrt{g'}}\right\} = \min\left\{1,\exp[-\beta(H_1'-H_1)]\left(\frac{\det[\mathbf{h}']}{\det[\mathbf{h}]}\right)^{d-1}\right\}, \quad (16)$$

where $H_1 = \Sigma_{i=1}^N \mathbf{p}_i^2/2m_i + (1/2W_g)\mathrm{Tr}[\mathbf{p}_g^t\mathbf{p}_g] + \phi + P_{\rm ext}\det[\mathbf{h}] + \frac{1}{2}\mathrm{Tr}[\Sigma G]$ and $\sqrt{g}$ is the metric factor associated with the phase-space compressibility of the non-Hamiltonian dynamics.[16,17] The latter is not unity only when the fully flexible cell is employed.

III. APPLICATION TO NI CRYSTAL

A. System and simulation details

In order to evaluate the efficiency of the four different schemes described above, i.e., NH-MD, NHC-MD, MNHC-MD, and HMC, we applied these methods to face-centered cubic (fcc) Ni crystal. This system consists of 500 Ni atoms in a three-dimensional periodic boundary cell. The EAM was used to model the interatomic interactions. Among several parametrizations of the EAM potential of the Ni system, the parameter set by Angelo *et al.*[24] was adopted here. This is a revised version originally developed by Daw and Baskes,[23] and by Foiles *et al.*,[25] which reproduce the experimental values well for the pure Ni properties, and was shown to be in good agreement with first-principles calculation.[32] The EAM being short range, no cutoff of the interaction was needed. During MD simulations, time-step size was fixed at 2 fs, and the fluctuation times of the barostat and thermostats were set to be 2 ps and 0.5 ps, respectively. In the HMC simulations, the step size is a tunable parameter to attain the efficient sampling of molecular configurations. Here we selected four step sizes 10 fs, 5 fs, 2 fs, and 1 fs to assess the efficiency of the HMC algorithm in estimating the elastic constants. Each MD simulation was carried out for 10 million steps. The first 1 million steps were the equilibration period, while the remaining 9 million steps were used in the sampling. Each HMC simulation was repeated for 1 million cycles, the first 0.1 million MC cycles was regarded as equilibration. The number of MD integration steps per Monte Carlo cycle, $n_{\rm MD/MC}$, which is also a tunable parameter in HMC, was fixed at 10. The cell parameters were stored every step in HMC, and every 10 steps in MD. Thus, we can compare the convergence properties of both the cell parameters and the elastic constants using the same statistics for MD and HMC. Throughout a series of simulations, the temperature was controlled at 300 K. Two conditions for the external stress were examined. The first examination was carried out under zero external stress. After this, the uniaxial tensile stress was applied stepwise to the system along the *x* axis by 1 GPa, up to 5 GPa. Then, the second examination was undertaken under the uniaxial tensile stress of $t_{xx}=5$ GPa.

B. Results

Figure 1 plots the cumulative average of the averaged cell length, $\langle L\rangle$, as a function of MD steps under the zero applied stress. All three MD simulations gave a fast convergence of the cell length, and the agreement among them was fairly good. In the case of HMC, however, the convergence property of the cell length was sensitive to the choice of the time-step size: As long as the step size less than 2 fs was used, the averaged cell length converged within a reasonable time, which was comparable to that of MD; whereas, using the step size of 10 fs, by which the acceptance probability of the HMC trial motion was about 45%, we observed a significant delay of the convergence of the cell length. In any case,

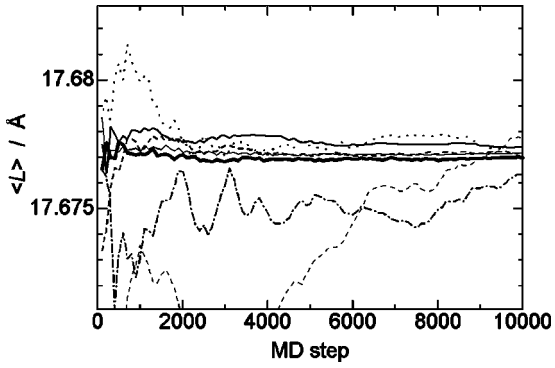

FIG. 1. Cumulative average of the cell length, $\langle L\rangle = V^{1/3}$, under the zero external stress. Thin solid line, NH-MD; solid line, NHC-MD; thick solid line, MNHC-MD; dotted line, HMC ($\Delta t=1$ fs); dashed line, HMC ($\Delta t=2$ fs), dash dotted line, HMC ($\Delta t=5$ fs); and thin dashed line; HMC ($\Delta t=10$ fs).

TABLE I. Averaged cell length and its statistical error under the zero external pressure (in angstrom). The latter was estimated by using the block averages with the length of 10^4 MD steps.

	H_{xx}	H_{yy}	H_{zz}
NH	17.67586($\pm$0.0015)	17.67420($\pm$0.0017)	17.67327($\pm$0.0017)
NHC	17.67511($\pm$0.0015)	17.67566($\pm$0.0015)	17.67428($\pm$0.0016)
MNHC	17.67606($\pm$0.0006)	17.67603($\pm$0.0006)	17.67611($\pm$0.0005)
HMC/10 fs	17.67582($\pm$0.0019)	17.67601($\pm$0.0020)	17.67587($\pm$0.0020)
HMC/5 fs	17.67613($\pm$0.0010)	17.67632($\pm$0.0010)	17.67592($\pm$0.0010)
HMC/2 fs	17.67669($\pm$0.0014)	17.67658($\pm$0.0014)	17.67659($\pm$0.0015)
HMC/1 fs	17.67679($\pm$0.0029)	17.67711($\pm$0.0028)	17.67648($\pm$0.0030)

however, all simulations produced a cell length converged to the same value within a small statistical error. In Table I, each component of the cell length averaged over the simulation time was listed with its statistical errors. The statistical error was estimated by using the block averages with each block length being 10^4 MD time steps. It is shown that, among all the algorithms employed here, MNHC-MD gives the best convergence with respect to the cell length. Under zero-stress condition, the cubic-cell symmetry, $\langle L_x\rangle = \langle L_y\rangle = \langle L_z\rangle$, should be satisfied. The numerical error for this condition is, again, the smallest in the MNHC simulation.

Figure 2 plots the cumulative average of the elastic constants C_{11}, C_{12}, and C_{44} (in Voigt notation), as a function of MD steps. Among three MD calculations, MNHC-MD clearly shows the best performance to attain well-converged elastic constants. For every component of elastic constants, cumulative averages are converged within about 1.5 million steps. The elastic constants obtained by NH- and NHC-MD approach rather slowly the same values that the MNHC-MD have settled. However, especially in C_{44}, NH-MD showed a poor convergence. On the other hand, the values of C_{11} and C_{12} obtained by HMC were quite sensitive to the choice of the time-step size. It was found that, with the shorter step size, those components showed the better agreement with the MD results. In contrast, the calculated C_{44}, C_{55}, and C_{66} (latter two are not shown in the figure) showed almost no dependence on the step size used in HMC simulations, being in good agreement with those obtained by MNHC-MD. In Table II, the overall average of elastic constants and their statistical errors were listed. The latter were estimated by using the block averages of the block length of 10^6 MD steps (10^5 data points). We can see from the table that MNHC-MD is always advantageous over NH- and NHC-MD in estimating the elastic constants efficiently within a small error. For comparison, the statistical errors of C_{11}, C_{12}, and C_{44} calculated by 10^5 MNHC-MD steps were 0.033, 0.046, and 0.013, which are comparable to those obtained by 10^6 NH-MD, respectively. Thus, MNHC-MD is more efficient than NH-MD by about one order of magnitude. In the calculation of elastic constants another point of concern is the symmetry of the elastic constants; in the case of the fcc nickel crystal under the zero stress, $C_{11}=C_{22}=C_{33}$, $C_{12}=C_{23}=C_{13}$, and $C_{44}=C_{55}=C_{66}$. However, for all the simulations studied here, numerical errors in these symmetries were smaller than the statistical error listed in Table II. In the table, the theoretical and experimental elastic constants are also listed. It was revealed that all simulations provided a lower value for the elastic constants than did the experimental measurements. The discrepancy would arise mainly from the inadequacy of the EAM parameters. It should be noted that the EAM parameters used here were fitted to room temperature rather than 0 K values for the elastic constants.[24] This explains the underestimation of the simulated values.

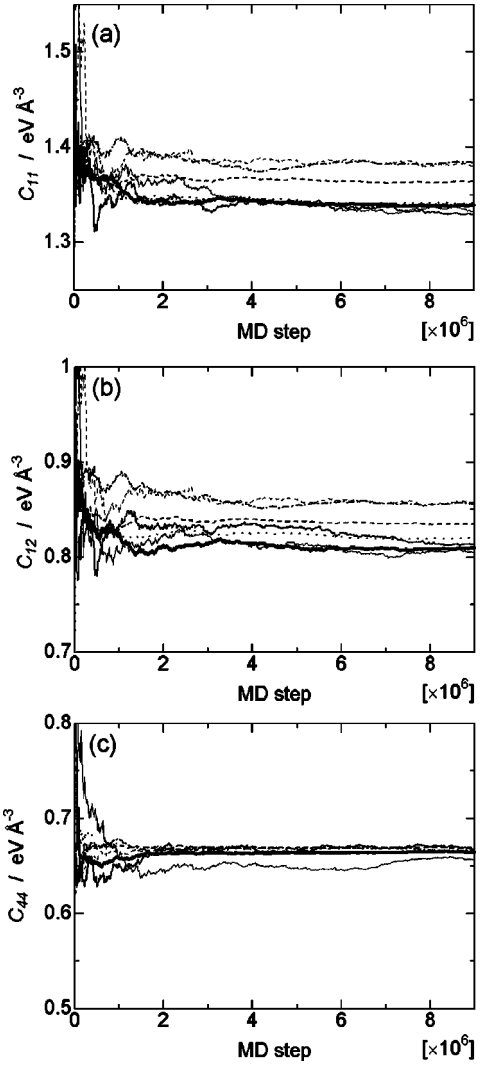

FIG. 2. Cumulative averages of the elastic constants under the zero external stress. (a) C_{11}, (b) C_{12}, and (c) C_{44}. Lines denote the same as in Fig. 1.

TABLE II. Elastic constants and their statistical errors under the zero external pressure (in eV $Å^{-3}$). The latter was estimated by using the block averages with the block length of 10^6 MD steps.

	C_{11}	C_{12}	C_{44}
NH	1.3331(±0.0150)	0.8051(±0.0134)	0.6568(±0.0115)
NHC	1.3304(±0.0111)	0.8137(±0.0130)	0.6678(±0.0090)
MNHC	1.3395(±0.0048)	0.8102(±0.0047)	0.6647(±0.0018)
HMC/10 fs	1.3822(±0.0066)	0.8572(±0.0071)	0.6659(±0.0018)
HMC/5 fs	1.3851(±0.0099)	0.8582(±0.0096)	0.6668(±0.0034)
HMC/2 fs	1.3638(±0.0051)	0.8347(±0.0042)	0.6691(±0.0014)
HMC/1 fs	1.3390(±0.0067)	0.8166(±0.0036)	0.6658(±0.0020)
Exp. [a]	1.54	0.92	0.78
Theory [a]	1.45	0.96	0.80

[a]Reference 25, and references therein. (In Ref. 25, the factor of 10^{12} must be missing due to a typological error.)

When the uniaxial tensile stress of 5 GPa was applied to the system, the results in the statistical convergence of elastic constants were similar to the previous zero-stress case. Figure 3 plots the cumulative average of the elastic constants under the uniaxial tensile stress $t_{xx}=5$ GPa and Table II shows the averaged data and the statistical errors estimated by using the block averages with the length of 10^6 MD steps trajectories. Again, the MNHC-MD has shown the best performance in estimating all the elastic constants (Table III). The HMC result of C_{11} and C_{12} largely depends on the MD step size for the trial motions. The smaller the step size in HMC sampling is, the better agreement between HMC and MC results is found.

IV. DISCUSSION

Our numerical tests have shown that MNHC-MD is advantageous over other simulation techniques studied here (NH-MD, NHC-MD, and HMC) in the estimation of both the cell parameters and the elastic constants. We will devote the last part of this paper to discuss possible reasons for this result and some methodological issues in these simulation techniques.

When we use a conventional Parrinello-Rahman's flexible cell MD method for solid-state systems, it is often observed that the system cannot reach canonical distribution even after a long time. This may be partly because the solid is generally a ''stiff'' system as to cell fluctuational motion. In a sense, it could be related to the famous problem for a single harmonic-oscillator system that canonical distribution is unable to reach within a simple system-thermostat coupling.[14] Nevertheless, a lot of MD studies that investigated the elastic constants of solids so far used this conventional algorithm and failed to make a precise evaluation of the elastic properties of the system. Instead, Monte Carlo simulations have been recently used to avoid this fault.[28,29] However, there are also demerit for MC; MC significantly decreases the sampling efficiency when the interatomic potential has a many-body nature or is estimated by a first-principles calculation, since the potential calculation will be time consuming for each trial move of one atom at a time. In addition, in the variety of applications of the mechanical analysis of some

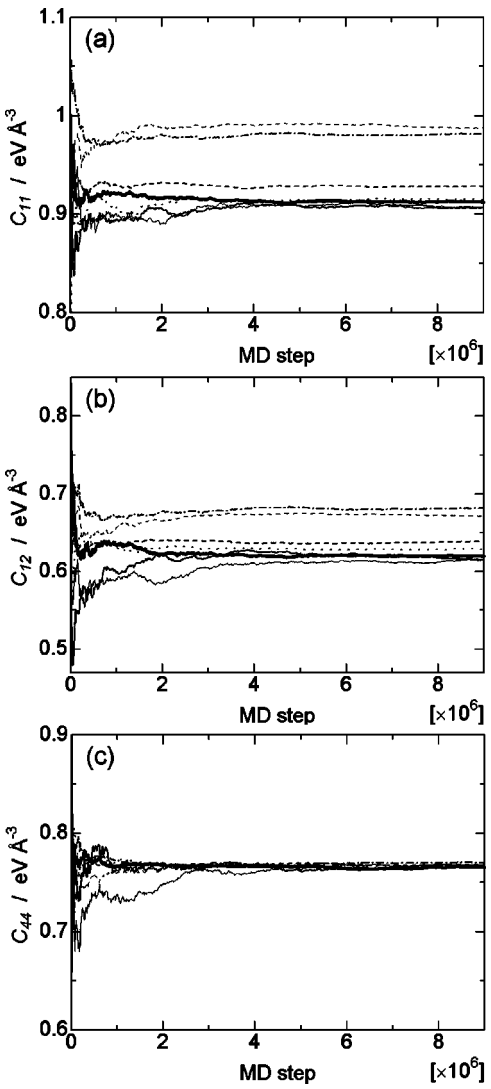

FIG. 3. Cumulative averages of the elastic constants under the uniaxial stress $\mathbf{t}_{xx}=-5$ GPa. (a) C_{11}, (b) C_{12}, and (c) C_{44}. Lines denote the same as in Fig. 1.

TABLE III. Elastic constants and their statistical errors under the uniaxial stress $\mathbf{t}_{xx}=-5$ GPa (in eV Å^{-3}). The latter was estimated by using the block averages with the block length of 10^6 MD steps.

	C_{11}	C_{22}	C_{12}	C_{23}	C_{44}	C_{55}
NH	0.9081($\pm$0.0091)	1.2573($\pm$0.0129)	0.6146($\pm$0.0097)	0.9425($\pm$0.0125)	0.7702($\pm$0.0086)	0.4539($\pm$0.0072)
NHC	0.9075($\pm$0.0053)	1.2611($\pm$0.0125)	0.6162($\pm$0.0092)	0.9431($\pm$0.0113)	0.7675($\pm$0.0077)	0.4575($\pm$0.0045)
MNHC	0.9124($\pm$0.0019)	1.2665($\pm$0.0043)	0.6200($\pm$0.0035)	0.9507($\pm$0.0051)	0.7659($\pm$0.0025)	0.4552($\pm$0.0015)
HMC/10 fs	0.9828($\pm$0.0022)	1.3016($\pm$0.0058)	0.6697($\pm$0.0033)	0.9906($\pm$0.0054)	0.7674($\pm$0.0046)	0.4535($\pm$0.0022)
HMC/5 fs	0.9817($\pm$0.0038)	1.3262($\pm$0.0063)	0.6817($\pm$0.0044)	1.0118($\pm$0.0064)	0.7704($\pm$0.0021)	0.4499($\pm$0.0020)
HMC/2 fs	0.9285($\pm$0.0024)	1.2873($\pm$0.0030)	0.6384($\pm$0.0023)	0.9736($\pm$0.0043)	0.7682($\pm$0.0018)	0.4563($\pm$0.0011)
HMC/1 fs	0.9145($\pm$0.0040)	1.2737($\pm$0.0031)	0.6283($\pm$0.0014)	0.9575($\pm$0.0043)	0.7665($\pm$0.0032)	0.4563($\pm$0.0030)

important materials, it is often critical to investigate the large-scale system that contains grain boundary or defects. To treat a large-scale system, MD is always advantageous over MC due to its feasibility of an efficient parallel computation. In the technical developments of MD methods, the NHC algorithm proposed to overcome the sampling problem indeed works well to give the canonical distribution for stiff system.[14] Furthermore, the MNHC algorithm, in which each degree of freedom in the system couples to a different NHC, may be expected to be efficient in estimating the elastic constants. Expectedly, this was confirmed in this study in the application to Ni crystal.

Originally, the MNHC algorithm was used in the path integral MD (PIMD) to attain the canonical distribution, since the stiff bond between the neighboring ''bead'' elements in a necklace gives rise to slow convergence of observable quantities.[33] The fact that the HMC algorithm is also successfully used in the PIMD encouraged us to use the HMC algorithm in our problem. Although the $N\mathbf{t}T$-HMC algorithm constructed on the basis of the non-Hamiltonian dynamics produces the same statistical average of the cell matrix, the calculated elastic constants C_{11} and C_{12}, depend sensitively on the choice of the step size.[34] In HMC, the step size Δt together with the number of MD steps per MC cycle, $n_{\mathrm{MD/MC}}$, are tunable parameters to attain the optimum efficiency in sampling the phase space. In our examination, $n_{\mathrm{MD/MC}}$ was fixed at 10 to compare HMC and MD with the same statistics (see Sec. III). If a larger $n_{\mathrm{MD/MC}}$ with a reasonably short step size is used in HMC, the calculated elastic constants, in principle, should approach to values obtained by MD. Actually, taking $n_{\mathrm{MD/MC}}=100$, we confirmed that HMC produced the same C_{11} and C_{12} as MD did, even if $\Delta t=10$ fs was used. However, using the long $n_{\mathrm{MD/MC}}$, the less data points are valid in sampling the cell matrix. Thus, a fast and accurate estimation of the elastic properties is not expected. In any case, HMC has a difficulty in choosing the simulation parameters $n_{\mathrm{MD/MC}}$ and Δt for the present purpose. In conclusion, MNHC-MD is a favorable algorithm in investigating the mechanical properties and stability of the solid materials by molecular simulations under an external stress.

ACKNOWLEDGMENTS

We are grateful to Dr. T. Ikeshoji and Dr. H. Kaburaki for helpful discussion.

*Electronic address: w.shinoda@aist.go.jp

[1] L. Yang, D.J. Srolovitz, and A.F. Yee, J. Chem. Phys. **107**, 4396 (1997).
[2] T. Çağin, G. Dereli, M. Uludogan, and M. Tomak, Phys. Rev. B **59**, 3468 (1999).
[3] G. Dereli, T. Çağin, M. Uludogan, and M. Tomak, Philos. Mag. Lett. **75**, 209 (1997).
[4] K.M. Aoki, M. Yoneya, and H. Yokoyama, J. Chem. Phys. **118**, 9926 (2003).
[5] J.S. Tse and D.D. Klug, Phys. Rev. Lett. **67**, 3559 (1991).
[6] J.R. Ray, Comput. Phys. Rep. **8**, 109 (1988).
[7] M. Parrinello and A. Rahman, J. Appl. Phys. **52**, 7182 (1981).
[8] M. Parrinello and A. Rahman, J. Chem. Phys. **76**, 2662 (1982).
[9] J. Wang and S. Yip, Phys. Rev. Lett. **71**, 4182 (1993).
[10] J. Wang, J. Li, and S. Yip, Phys. Rev. B **52**, 12 627 (1995).
[11] Z. Zhou and B. Joós, Phys. Rev. B **54**, 3841 (1996).
[12] J.R. Ray and A. Rahman, J. Chem. Phys. **80**, 4423 (1984).
[13] M. Sprik, R.W. Impey, and M.L. Klein, Phys. Rev. B **29**, 4368 (1984).
[14] G.J. Martyna, M.L. Klein, and M. Tuckerman, J. Chem. Phys. **97**, 2635 (1992).
[15] B. Mehlig, D.W. Heermann, and B.M. Forrest, Phys. Rev. B **45**, 679 (1992).
[16] M.E. Tuckerman, C.J. Mundy, and G.J. Martyna, Europhys. Lett. **45**, 149 (1999).
[17] M.E. Tuckerman, Y. Liu, G. Ciccotti, and G.J. Martyna, J. Chem. Phys. **115**, 1678 (2001).
[18] G.J. Martyna, D.J. Tobias, and M.L. Klein, J. Chem. Phys. **101**, 4177 (1994).
[19] M. Tuckerman, G.J. Martyna, and B.J. Berne, J. Chem. Phys. **97**, 1990 (1992).
[20] G.J. Martyna, M.E. Tuckerman, D.J. Tobias, and M.L. Klein, Mol. Phys. **87**, 1117 (1996).
[21] S. Nosé, Mol. Phys. **52**, 255 (1984); S. Nosé, J. Chem. Phys. **81**, 511 (1984).
[22] W.G. Hoover, Phys. Rev. A **31**, 1695 (1985).
[23] M.S. Daw and M.I. Baskes, Phys. Rev. Lett. **50**, 1285 (1983); Phys. Rev. B **29**, 6443 (1984).

[24] J.E. Angelo, N.R. Moody, and M.I. Baskes, Modell. Simul. Mater. Sci. Eng. **3**, 289 (1995); M.I. Baskes, X. Sha, J.E. Angelo, and N.R. Moody, *ibid.* **5**, 651 (1997).
[25] S.M. Foiles, M.I. Baskes, and M.S. Daw, Phys. Rev. B **33**, 7983 (1986); S.M. Foiles, M.I. Baskes, C.F. Melius, and M.S. Daw, J. Less-Common Met. **130**, 465 (1987).
[26] M. Karimi, G. Stapay, T. Kaplan, and M. Mostoller, Modell. Simul. Mater. Sci. Eng. **5**, 337 (1997).
[27] T. Çağin and B.M. Pettitt, Phys. Rev. B **39**, 12 484 (1989).
[28] P.J. Fay and J.R. Ray, Phys. Rev. A **46**, 4645 (1992).
[29] M. Karimi, H. Yates, J.R. Ray, T. Kaplan, and M. Mostoller, Phys. Rev. B **58**, 6019 (1998).
[30] W. Zhong, Y. Cai, and D. Tomanek, Phys. Rev. B **46**, 8099 (1992).
[31] R.J. Wolf, K.A. Mansour, M.W. Lee, and J.R. Ray, Phys. Rev. B **46**, 8027 (1992).
[32] M. Shiga, M. Yamaguchi, and H. Kaburaki, Phys. Rev. B **68**, 245402 (2003).
[33] M.E. Tuckerman and A. Hughes, in *Classical and Quantum Dynamics in Condensed Phase Simulations*, edited by B.J. Berne, G. Ciccotti, and D.F. Coker (World Scientific, Singapore, 1998), p. 311.
[34] We confirmed that MD algorithms used in this work showed no dependency on the step size as long as it is short enough; when $\Delta t = 1$ fs, the calculated elastic constants accorded with those obtained by $\Delta t = 2$ fs within the statistical errors.